Refinement of a design-oriented stress-strain model for FRP-confined concrete

J.G. Teng[1,*], T. Jiang[1], L. Lam[1] and Y.Z. Luo[2]

[1]Department of Civil and Structural Engineering
The Hong Kong Polytechnic University, Hong Kong, China
[2]Department of Civil Engineering
Zhejiang University, Hangzhou, Zhejiang Province, China
*cejgteng@polyu.edu.hk

Abstract: This paper presents the results of a recent study conducted to refine the design-oriented stress-strain model originally proposed by Lam and Teng for FRP-confined concrete under axial compression. More accurate expressions for the ultimate axial strain and the compressive strength are proposed for use in this model. These new expressions are based on results from recent tests conducted by the authors' group under well-defined conditions and on results from a parametric study using an accurate analysis-oriented stress-strain model for FRP-confined concrete. They allow the effects of confinement stiffness and the jacket strain capacity to be separately reflected and accounts for the effect of confinement stiffness explicitly instead of having it reflected only through the confinement ratio. The new expressions can be easily incorporated into Lam and Teng's model for more accurate predictions. Based on these new expressions, two modified versions of Lam and Teng's model are presented. The first version involves only the updating of the ultimate axial strain and compressive strength equations. The second version caters for stress-strain curves with a descending branch, which is not covered by the original model.

Keywords: FRP; concrete; confinement; stress-strain model; design

1   Introduction

Various stress-strain models have been developed for fiber reinforced polymer (FRP)-confined concrete under axial compression. These models can be classified into two main categories (Teng and Lam 2004): design-oriented models (e.g. Fardis and Khalili 1982; Karbhari and Gao 1997; Samaan et al. 1998; Miyauchi et al. 1999; Saafi et al. 1999; Toutanji 1999; Lillistone and Jolly 2000; Xiao and Wu 2000, 2003; Lam and Teng 2003; Berthet et al. 2006; Harajli 2006; Saenz and Pantelides 2007; Wu et al. 2007; Youssef et al. 2007) and analysis-oriented models (e.g. Mirmiran and Shahawy 1997; Spoelstra and Monti 1999; Fam and Rizkalla 2001; Chun and Park 2002; Harries and Kharel 2002; Marques et al. 2004; Binici 2005; Teng et al. 2007a; Jiang and Teng 2007). Design-oriented models are generally defined using simple closed-form expressions and are suitable for direct use in practical design. By contrast, analysis-oriented models generally predict stress-strain curves using an incremental-iterative procedure and are thus undesirable for direct use in design.

Analysis-oriented models have a better predictive capability and are more versatile than designed-oriented models as the former account explicitly for the interaction between the confining material and the concrete core. Therefore, a rational approach for the development of a design-oriented model is to base it on extensive numerical results from an accurate

analysis-oriented model in addition to a more limited set of test results. A comprehensive review and assessment of existing analysis-oriented models has recently been conducted by Jiang and Teng (2007) who also showed that Teng et al.'s (2007a) model, with a modification proposed by them, can provide accurate predictions of test results.

Among the many different design-oriented stress-strain models, the model proposed by Lam and Teng (2003) appears to be advantageous over other models due to its simple and familiar form as well as accuracy. This model, with some modification, has been adopted by the design guidance for the strengthening of concrete structures using FRP issued by the Concrete Society (2004) in the UK. More recently, this model has also been adopted by ACI-440.2R (2008) with only very slight modifications. The model adopts a simple form that naturally reduces to that for unconfined concrete when no FRP is provided. Its simple form also caters for easy improvements to the definition of the ultimate condition (the ultimate axial strain and the compressive strength) of FRP-confined concrete, which are the key to the accurate prediction of stress-strain curves of FRP-confined concrete by this model.

Although Lam and Teng's (2003) model was developed on the basis of a large database of tests on FRP-confined circular concrete cylinders, a number of significant issues could not be readily resolved using the test database available to them at that time. In particular, there was considerable uncertainty with the hoop tensile strain reached by the FRP jacket at rupture failure, which has an important bearing on the definition of the ultimate condition. According to a subsequent study by the same authors (Lam and Teng 2004), the distribution of FRP hoop strains is highly non-uniform around the circumference of an FRP-confined concrete cylinder and the hoop strains in the overlapping zone of the FRP jacket are much lower than those measured elsewhere. The lower FRP hoop strains in the overlapping zone reduce the average hoop strain but do not result in a lower confining pressure in this zone because the FRP jacket is thicker there (Lam and Teng 2004). This observation suggests that hoop strain readings within the overlapping zone should be excluded when interpreting the behavior of FRP-confined concrete, as these readings reflect neither the actual strain capacity of the confining jacket nor the actual dilation properties of the confined concrete. However, such important processing of the hoop strain readings was not possible with test data collected by Lam and Teng (2003) from the existing literature at that time, for which the precise number and locations of strain gauges for measuring hoop strains were generally not reported. Apart from the uncertainty associated with the FRP hoop strain, the different methods of axial strain measurements (e.g. strain gauges versus displacement transducers and the gauge lengths employed) adopted by different researchers may have also affected the consistency of the test data of that database.

To address these deficiencies of that database and hence those of Lam and Teng's (2003) stress-strain model, a large number of additional tests on FRP-confined concrete cylinders have been conducted under standardized testing conditions by the authors' group (Lam and Teng 2004, Lam et al. 2006, Teng et al. 2007b, Jiang and Teng 2007). In addition, further theoretical modeling work on FRP-confined concrete has also been carried out by the authors' group (Teng et al. 2007a; Jiang and Teng 2007). These recent test results and the new understandings from further research have accumulated a solid basis for the refinement of Lam and Teng's (2003) stress-strain model.

This paper therefore presents refinements to the Lam and Teng (2003) stress-strain model. In this paper, more accurate expressions for the ultimate axial strain and the compressive strength of FRP-confined concrete are first developed. Two modified versions of Lam and

Teng's model based on these new expressions are next presented. The first version involves only the updating of the ultimate condition equations. The second version differs from the first version in that it is capable of predicting stress-strain curves with a descending branch when the level of confinement is low.

It should be noted that in this paper, the term "stress-strain" should be understood as "axial stress-axial strain". The latter is used only when the axial stress-lateral strain responses of the concrete are also discussed. The following sign convention is adopted: in the concrete, compressive stresses and strains are positive, but in the FRP, tensile stresses and strains are positive.

2 Test database

2.1 General

The test database used in the present study (i.e. the present test database) has previously been reported by Jiang and Teng (2007) for the assessment of analysis-oriented stress-strain models. This database contains results of 48 tests on concrete cylinders (152 mm × 305 mm) confined with varying amounts of carbon FRP (CFRP) and Glass FRP (GFRP), with the unconfined concrete strength (i.e. the compressive strength of unconfined concrete) $f_{co}^{'}$ ranging from 33.1 MPa to 47.6 MPa. All these tests were recently conducted under standardized test conditions at The Hong Kong Polytechnic University by the authors' group. As full details of these tests are available in Jiang and Teng (2007), only the key features of the test database are summarized below:

a) The FRP jackets were formed via the wet lay-up process and had hoop fibers only. For each batch of concrete, two or three 152 mm x 305 mm plain concrete cylinders were tested as control specimens to determine the average values of the unconfined concrete strength $f_{co}^{'}$ and the corresponding axial strain ε_{co}.

b) The hoop strain ε_h of the FRP jacket was found as the average reading of the five hoop strain gauges outside the 150 mm overlapping zone; these gauges had a 20 mm gauge length.

c) The axial strain of concrete ε_c was found as the average reading of two linear variable displacement transducers (LVDTs) at 180° apart and covering the mid-height region of 120 mm. The lateral strain of concrete ε_l was assumed to be equal to the jacket hoop strain in magnitude; they have different signs according to the adopted sign convention.

d) The test database covers a wide range of FRP confinement levels. The compressive strength of the most heavily-confined specimen increased by about 320% due to confinement while the most lightly-confined specimen exhibited a stress-strain curve with a descending branch and a negligible strength increase.

For ease of discussion, three basic ratios are first defined: the confinement ratio $f_l / f_{co}^{'}$, the confinement stiffness ratio ρ_K and the strain ratio ρ_ε. The mathematical expressions of these three ratios are as follows:

$$\frac{f_l}{f_{co}^{'}} = \frac{2E_{frp}t\varepsilon_{h,rup}}{f_{co}^{'}D} = \rho_K \rho_\varepsilon \qquad (1a)$$

$$\rho_K = \frac{2E_{frp}t}{\left(f_{co}^{'}/\varepsilon_{co}\right)D} \tag{1b}$$

$$\rho_\varepsilon = \frac{\varepsilon_{h,rup}}{\varepsilon_{co}} \tag{1c}$$

where f_l is the confining pressure provided by the FRP jacket when it fails by rupture due to hoop tensile stresses (i.e. the maximum confining pressure possible with the jacket), E_{frp} is the elastic modulus of FRP in the hoop direction, t is the thickness of the FRP jacket, $\varepsilon_{h,rup}$ is the hoop rupture strain of the FRP jacket, and D is the diameter of the confined concrete cylinder. The confinement ratio is a commonly used parameter in the existing literature. The confinement stiffness ratio represents the stiffness of the FRP jacket relative to that of the concrete core. The strain ratio is a measure of the strain capacity of the FRP jacket. The confinement ratio is equal to the product of the other two ratios.

2.2 Stress-strain curves

The stress-strain curves as well as other key results of all these tests are given in Jiang and Teng (2007). Only eight typical stress-strain curves are shown in Fig. 1 to illustrate the behavior of confined concrete cylinders. Both the axial strain ε_c and the lateral strain ε_l are normalized by the corresponding value of ε_{co}, while the axial stress σ_c is normalized by the corresponding value of $f_{co}^{'}$. All the ascending type curves in Fig. 1 exhibit the well-known bi-linear shape, ending with the rupture of the confining jacket at the ultimate point defined by the compressive strength $f_{cc}^{'}$ and the ultimate axial strain ε_{cu}; both the strength and the strain capacity of the concrete are significantly enhanced. By contrast, for the descending type stress-strain curves, $f_{cc}^{'}$ is reached before the rupture of the jacket with very limited strength enhancement. For ease of discussion, if the axial stress of FRP-confined concrete at ultimate axial strain $f_{cu}^{'}$ falls below the unconfined concrete strength $f_{co}^{'}$, the concrete is classified as insufficiently confined in this paper. All other cases of FRP-confined concrete are classified as sufficiently confined. The key information of these eight specimens, together with that of some other specimens referred to in the present paper, is given in Table 1. The names of the specimens are the same as reported in Jiang and Teng (2007).

2.3 Ultimate condition

Using the analysis-oriented model for FRP-confined concrete proposed by Spoelstra and Monti (1999), Lam and Teng (2003) demonstrated that the stiffness of the FRP jacket affects both the ultimate axial strain and the compressive strength of FRP-confined concrete. The tests of the present database offer clear experimental evidence on the effect of jacket stiffness, as illustrated in Fig. 2. Fig. 2a shows the experimental stress-strain curves of specimens 31 and 45. The former had an unconfined concrete strength of 45.9 MPa, a GFRP jacket, and a confinement ratio of 0.140, while the latter had an unconfined concrete strength of 44.2 MPa, a CFRP jacket and a confinement ratio of 0.141. It can be seen that although the two specimens had very similar unconfined concrete strengths and confinement ratios, their stress-strain curves are significantly different in the later stage due to the difference in the jacket confinement stiffness. The stress-strain curve of specimen 31 with a smaller confinement stiffness ratio terminates at a lower axial stress but a larger axial strain.

Similarly, Fig. 2b shows the stress-strain curves of specimens 28 and 42. The former had an unconfined strength of 45.9 MPa and a confinement ratio of 0.059 while the latter had an unconfined strength 44.2 MPa and a confinement ratio of 0.055. It is interesting to note that specimen 28 with a smaller confinement stiffness ratio exhibited a stress-strain curve of the descending type while specimen 42 exhibited a stress-strain curve of the ascending type. These observations suggest that the effect of confinement stiffness on the ultimate condition of FRP-confined concrete should be properly reflected in a design-oriented stress-strain model. The comparison shown in Fig. 2b also suggests that the confinement stiffness ratio is important in determining whether the sufficient confinement condition is met.

3   Lam and Teng's stress-strain model for FRP-confined concrete

Lam and Teng's (2003) design-oriented stress-strain model is based on the following assumptions: (i) the stress-strain curve consists of a parabolic first portion and a linear second portion, as illustrated in Fig. 3; (ii) the slope of the parabola at zero axial strain (the initial slope) is the same as the elastic modulus of unconfined concrete; (iii) the nonlinear part of the first portion is affected to some degree by the presence of an FRP jacket; (iv) the parabolic first portion meets the linear second portion smoothly (i.e. there is no change in slope between the two portions where they meet); (v) the linear second portion terminates at a point where both the compressive strength and the ultimate axial strain of confined concrete are reached; and (vi) the linear second portion intercepts the axial stress axis at a stress value equal to the unconfined concrete strength. The justifications for the above assumptions are given in Lam and Teng (2003) and are thus not repeated herein.

Based on these assumptions, Lam and Teng's stress-strain model for FRP-confined concrete is described by the following expressions:

$$\sigma_c = E_c \varepsilon_c - \frac{\left(E_c - E_2\right)^2}{4 f_{co}^{'}} \varepsilon_c^2 \quad \text{for} \quad 0 \le \varepsilon_c < \varepsilon_t \tag{2a}$$

$$\sigma_c = f_{co}^{'} + E_2 \varepsilon_c \quad \text{for} \quad \varepsilon_t \le \varepsilon_c \le \varepsilon_{cu} \tag{2b}$$

where σ_c and ε_c are the axial stress and the axial strain respectively, E_c is the elastic modulus of unconfined concrete, and E_2 is the slope of the linear second portion. The parabolic first portion meets the linear second portion with a smooth transition at ε_t which is given by

$$\varepsilon_t = \frac{2 f_{co}^{'}}{E_c - E_2} \tag{3}$$

The slope of the linear second portion E_2 is given by

$$E_2 = \frac{f_{cc}^{'} - f_{co}^{'}}{\varepsilon_{cu}} \tag{4}$$

This model allows the use of test values or values specified by design codes for the elastic modulus of unconfined concrete E_c. Lam and Teng (2003) proposed the following equation to predict the ultimate axial strain ε_{cu} of confined concrete:

$$\frac{\varepsilon_{cu}}{\varepsilon_{co}} = 1.75 + 12\rho_K \rho_\varepsilon^{1.45} \tag{5}$$

Lam and Teng's (2003) compressive strength equation takes the following form:

$$\frac{f_{cc}^{'}}{f_{co}^{'}} = 1 + 3.3\frac{f_l}{f_{co}^{'}} \text{ , if } \frac{f_l}{f_{co}^{'}} \geq 0.07 \tag{6a}$$

$$\frac{f_{cc}^{'}}{f_{co}^{'}} = 1 \text{, if } \frac{f_l}{f_{co}^{'}} < 0.07 \tag{6b}$$

Eqs 6a and 6b are for sufficiently and insufficiently confined concrete respectively. A minimum value of 0.07 for $f_l / f_{co}^{'}$ for sufficient confinement was originally suggested by Spoelstra and Monti (1999) and was used in Lam and Teng's (2003) model with justification using test data available to them.

A comparison of Lam and Teng's model with the test data of the present database is shown in Fig. 4. In predicting the compressive strength and the ultimate axial strain, a constant value of 0.002 for ε_{co} was used. The experimental values of $\varepsilon_{h,rup}$ were used in making the predictions shown in Fig.4 and throughout the paper. The elastic modulus of unconfined concrete was taken to be $E_c = 4730\sqrt{f_{co}^{'}}$ (in MPa) [ACI-318 (2005)]. It can be seen from Fig. 4 that Eqs 5 and 6 overestimate the ultimate axial strain of concrete at high levels of confinement and the compressive strength of concrete at low levels of confinement. In addition, the effect of confinement stiffness is only explicitly and separately accounted for in the ultimate axial strain equation, but not in the compressive strength equation. Refinement of these equations is therefore necessary to provide more accurate predictions.

4 Generalization of equations

To take the effect of confinement stiffness into proper account, the expressions for the ultimate axial strain and the compressive strength of FRP-confined concrete are generalized here. Eq. 5 can be cast into the following form:

$$\frac{\varepsilon_{cu}}{\varepsilon_{co}} = C_\varepsilon + F_\varepsilon(\rho_K)f_\varepsilon(\rho_\varepsilon) \tag{7}$$

where $F_\varepsilon(\rho_K)$ and $f_\varepsilon(\rho_\varepsilon)$ are functions of the confinement stiffness ratio and strain ratio respectively, and C_ε is a constant.

Since the confinement ratio is the product of the confinement stiffness ratio and the strain ratio, Eq. 6 can be cast into the following form which is similar to Eq. 7:

$$\frac{f_{cc}^{'}}{f_{co}^{'}} = C_{\sigma} + F_{\sigma}(\rho_{K})f_{\sigma}(\rho_{\varepsilon}) \tag{8}$$

where $F_{\sigma}(\rho_{K})$ and $f_{\sigma}(\rho_{\varepsilon})$ are also functions of the confinement stiffness ratio and the strain ratio respectively, and C_{σ} is a constant.

The above generalization allows the effects of confinement stiffness and the jacket strain capacity to be separately reflected in both the ultimate axial strain and the compressive strength equations and accounts for the effect of confinement stiffness explicitly instead of having it reflected only through the confinement ratio.

5   New equations for the ultimate condition

5.1   Ultimate axial strain

Based mainly on the interpretation of the test results in the present database, the following improved equation for the ultimate axial strain of FRP-confined concrete is proposed:

$$\frac{\varepsilon_{cu}}{\varepsilon_{co}} = 1.75 + 6.5\rho_{K}^{0.8}\rho_{\varepsilon}^{1.45} \tag{9}$$

where the strain at the unconfined concrete strength ε_{co} was taken to be 0.002 in determining the strain ratio ρ_{ε}, since this value is commonly accepted in existing design codes for concrete structures. It is therefore suggested that this value should be used when the proposed model is used in design. The first term on the right-hand side of Eq. 9 is taken to be 1.75 so that the equation predicts a value of 0.0035 for ε_{cu} when no FRP confinement is provided; the coefficient/exponents within the second term were determined by regression analysis of the present test results. It should be noted that $\varepsilon_{cu} = 0.0035$ is commonly accepted for unconfined concrete; the constant 1.75 may be adjusted to suit a different value for the ultimate axial strain of unconfined concrete in a specific design code. In Fig. 5, the predictions of Eq. 9 are compared with the present test database as well as the test database assembled by Lam and Teng (2003) on which the previous version of the ultimate condition equations (Eqs 5 and 6) was based. Lam and Teng's (2003) test database contains 76 non-identical specimens from 14 independent sources. These specimens had diameters ranging from 100 mm to 200 mm and unconfined concrete strengths ranging from 26.2 to 55.2 MPa. Fig. 5 shows that Eq. 9 is very accurate for the present test database. The results of Lam and Teng's (2003) database are nicely scattered around the predictions (particularly in the lower range of ultimate axial strains where there are more test data points), confirming the general validity of the new ultimate axial strain equation; the wide scatter of these test data are attributed to the deficiencies of that database as discussed earlier in this paper.

5.2   Compressive strength

The compressive strength equation was refined on a combined experimental and analytical basis. Fig. 1 shows that both the axial stress-lateral strain curves and the axial stress-axial strain curves exhibit a bi-linear shape, with the two portions smoothly connected by a transition zone near the unconfined concrete strength. The shape of the second portion is very close to a straight line. Fig. 1 also shows that the second portion of an axial stress-lateral

strain curve is closer to being a straight line than that of an axial stress-axial strain curve. A careful examination of the present tests data showed that the second portion of all the experimental axial stress-lateral strain curves intercepts the axial stress axis at a stress value which is very close to the unconfined concrete strength when this portion is approximated by a best-fit straight line. These straight lines can be represented by the following equation:

$$\frac{\sigma_c}{f_{co}'} = 1 + K \frac{\varepsilon_l}{\varepsilon_{co}} \tag{10}$$

which means that the constant C_σ in Eq. 8 has been taken to be unity for the reason given above. K is the slope of the fitted straight line. It is obvious that the axial stress σ_c reaches f_{cu}' when $\varepsilon_l = -\varepsilon_{h,rup}$, and Eq. 10 thus becomes

$$\frac{f_{cu}'}{f_{co}'} = 1 - K \frac{\varepsilon_{h,rup}}{\varepsilon_{co}} = 1 - K \rho_\varepsilon \tag{11}$$

Comparing Eq. 11 with Eq. 8 leads to $F_\varepsilon(\rho_\varepsilon) = \rho_\varepsilon$ while the slope $K = F_\sigma(\rho_K)$ is yet to be determined.

To define $F_\sigma(\rho_K)$ in Eq. 11, a parametric study was conducted using the refined version (Jiang and Teng 2007) of the analysis-oriented stress-strain model of Teng et al. (2007a) for FRP-confined concrete. The parametric study covered concrete cylinders of 152 mm in diameter and confined with either CFRP or GFRP, with f_{co}' ranging from 20 to 50 MPa and a wide range of jacket thicknesses to represent different values of confinement stiffness. The material properties used and parameters studied are given in Table 2. In the parametric study, it was assumed $\varepsilon_{co} = 9.37 \times 10^{-4} \sqrt[4]{f_{co}'}$ (Popovics 1973) instead of the more approximate value of 0.002. The value of ε_{co} has some effect on the accuracy of this analysis-oriented model, so Jiang and Teng (2007) suggested the use of this expression for cases where the value of ε_{co} has to be assumed, for instance, in a parametric study. The parametric study consisted of three steps: 1) produce a family of axial stress-lateral strain curves of a concrete cylinder confined with a certain type of FRP jacket for different confinement stiffness ratios; 2) approximate the second portions of these axial stress-lateral strain curves using best-fit straight lines that intercept the vertical axis ($\frac{\sigma_c}{f_{co}'}$) at unity; and 3) identify $F_\sigma(\rho_K)$ by finding the relationship between the slopes of these straight lines and the confinement stiffness ratios.

Fig. 6a demonstrates the first two steps for a concrete cylinder with $f_{co}' = 30$ MPa confined with a CFRP jacket for a range of jacket thicknesses. Each stress-strain curve in Fig. 6a corresponds to a particular value of the confinement stiffness ratio. The portions of the stress-strain curves from $\varepsilon_l = -0.5\varepsilon_{co}$ onwards were fitted using straight lines (dashed lines in Fig. 6a). The slopes of the fitted lines are shown against the confinement stiffness ratios in Fig. 6b, as a demonstration of the last step. A corresponding curve for the same concrete cylinder but with GFRP confinement is also shown in Fig. 6b. It can be seen that these two curves are almost identical and can be closely represented using the following expression:

$$K = F_\sigma(\rho_K) = -3.2\rho_K^{0.9} + 0.06 \qquad (12)$$

Eq. 12 also provides accurate predictions for other values of f_{co}' studied. With $F_\sigma(\rho_K)$ defined, Eq. 11 becomes

$$\frac{f_{cu}'}{f_{co}'} = 1 + \left(3.2\rho_K^{0.9} - 0.06\right)\rho_\varepsilon \qquad (13)$$

Fig. 7 shows that Eq. 13 compares well with the present test results. In predicting f_{cu}' for Fig. 7, experimental values of ε_{co} were used, as the aim was to verify the accuracy of Eq. 13 using experiments.

As the nonlinear relationship between $F_\sigma(\rho_K)$ and ρ_K in Eq. 13 is slightly inconvenient for design use, the following simple linear equation is proposed as an approximation:

$$\frac{f_{cu}'}{f_{co}'} = 1 + 3.5\left(\rho_K - 0.01\right)\rho_\varepsilon \qquad (14)$$

It should be noted that Eq. 14 predicts the axial stress at the ultimate axial strain, but not the compressive strength f_{cc}' of FRP-confined concrete, although they are the same unless the stress-strain curve features a descending branch. Since Lam and Teng's (2003) model neglects the small amount of strength enhancement in insufficiently confined concrete and employs a horizontal line to approximate the descending branch of such concrete, Eq. 14 needs to be modified for direct incorporation into Lam and Teng's model (2003) for predicting f_{cc}'. It is proposed that

$$\frac{f_{cc}'}{f_{co}'} = 1 + 3.5\left(\rho_K - 0.01\right)\rho_\varepsilon \text{, if } \rho_K \geq 0.01 \qquad (15a)$$

$$\frac{f_{cc}'}{f_{co}'} = 1 \text{, if } \rho_K < 0.01 \qquad (15b)$$

The performance of Eq. 15 as assessed using the present test database and Lam and Teng's (2003) test database is shown in Fig. 8. Eq. 15 is seen to provide accurate predictions of the results of the present test data. For the results of Lam and Teng's (2003) database, Eq. 5 becomes more conservative but still compares well with the test results. In predicting f_{cc}' for Fig. 8, $\varepsilon_{co} = 0.002$ was used for assessing the accuracy of Eq. 15 in design applications. Eq. 15 defines a minimum confinement stiffness ratio ρ_K of 0.01 below which the FRP is assumed to result in no enhancement in the compressive strength of concrete.

It should be noted that the above comparisons for the new ultimate condition equations are based on small-scale specimens with diameters ranging from 100 mm to 200 mm. Specimens of such sizes have been used in the vast majority of existing studies on the stress-strain behavior of FRP-confined concrete. Only a small number of experimental studies have been

conducted on the axial compressive behavior of large-scale circular columns (Youssef 2003; Carey and Harries 2005; Mattys et al. 2005; Rocca et al. 2006; Yeh and Chang 2007). In these few studies, columns with a diameter up to 610 mm were tested and the test results indicated that within this range, the stress-strain behavior does not vary significantly with the column diameter. The effect of column size is thus believed to be limited for circular columns.

6   Modifications to Lam and Teng's model-Version I

Eqs 9 and 15 can be directly incorporated into Lam and Teng's (2003) model. Fig. 9 shows a comparison between the predictions of the original model and those of the modified model (referred to as Version I to differentiate it from Version II presented in the next section) for three sets of specimens of the present test database. The first two sets of specimens (specimens 22 and 23 in Fig. 9a and specimens 24 and 25 in Fig. 9b) had an unconfined concrete strength of 39.6 MPa and were confined with 2 and 3 plies of GFRP, respectively. The confinement ratio is 0.186 for the 2-ply GFRP jacket and 0.278 for the 3-ply GFRP jacket, while the confinement stiffness ratio is 0.018 for the former and 0.027 for the latter. The last set of specimens (specimens 17, 18 and 19 in Fig 8c) had an unconfined concrete strength of 38.9 MPa and were confined with 2 plies of CFRP, with a confinement ratio of 0.274 and a confinement stiffness ratio of 0.055. The predicted stress-strain curves were obtained using $\varepsilon_{co} = 0.002$.

It is evident that the original model provides close predictions for the specimens with two plies of CFRP (Fig. 9c), but not for those with two and three plies of GFRP (Figs 9a and 9b). Note that the confinement ratio of the 3-ply GFRP jacket is similar to that of the 2-ply CFRP jacket (0.278 versus 0.274), but the confinement stiffness ratio of the former (0.027) is only half that of the latter (0.055). The inaccuracy of the original model in this case is due to the omission of the confinement stiffness as a parameter in addition to the confining pressure in the compressive strength equation (Eq. 6). It is clear that the use of Eqs 9 and 15 in Lam and Teng's (2003) model improves its performance considerably for cases of low confinement stiffness ratios.

7   Modifications to Lam and Teng's model-Version II

Both the original model of Lam and Teng (2003) and the modified version presented above simply approximate a post-peak descending branch due to a low level of confinement using a horizontal line. As a result, when no FRP confinement is present, the second branch of Lam and Teng's model reduces directly to the second branch of stress-strain models for unconfined concrete in many existing design codes for concrete structures such as Eurocode 2 (ENV 1992-1-1 1991) although the ultimate strain value in each code may be slightly different. This is clearly an advantage.

However, in applications where ductility is the main concern, this simple approach may not be satisfactory. For example, in the seismic retrofit of concrete columns, a small amount of FRP confinement may be sufficient in enhancing the ductility of concrete although it is not sufficient to result in a significant enhancement in compressive strength. In such a situation, a more precise definition of the post-peak stress-strain response of FRP-confined concrete is of interest to structural engineers. For this reason, another modified version, referred to as Version II, of Lam and Teng's model is proposed in this section.

In order to cater for both the ascending and descending types of stress-strain curves of FRP-confined concrete, the stress-strain curve of unconfined concrete for design use is defined in a form similar to the well-known Hognestad's (1951) stress-strain curve. It is assumed that the stress-strain curve of unconfined concrete has a linear post-peak descending branch, which terminates at an axial strain of 0.0035 after a 15% drop from the compressive strength of unconfined concrete. Note that in Hognestad's (1951) model, the ultimate axial strain of unconfined concrete was defined as 0.0038, instead of 0.0035. The latter is specified in design codes such as BS 8110 (1997) and ENV 1992-1-1 (1991).

In this alternative version, the parabolic first portion of Lam and Teng's model as given by Eq. 1a remains unchanged, while the linear second portion given by Eq. 1b is modified, leading to the following expressions:

$$\sigma_c = \begin{cases} E_c \varepsilon_c - \dfrac{(E_c - E_2)^2}{4 f_{co}'} & (0 \le \varepsilon_c \le \varepsilon_t) \\[2mm] \begin{cases} f_{co}' + E_2 \varepsilon_c & \text{if } \rho_K \ge 0.01 \\[2mm] f_{co}' - \dfrac{f_{co}' - f_{cu}'}{\varepsilon_{cu} - \varepsilon_{co}}(\varepsilon_c - \varepsilon_{co}) & \text{if } \rho_K < 0.01 \end{cases} & (\varepsilon_t < \varepsilon_c \le \varepsilon_{cu}) \end{cases} \tag{16}$$

where E_2, ε_{cu} and f_{cc}' are defined by Eqs 4, 9 and 15 respectively, and f_{cu}' is given by Eq. 14 but is subjected to the following conditions:

$$f_{cu}' \ge 0.85 f_{co}', \text{ if } \rho_K > 0; \text{ or } = 0.85 f_{co}', \text{ if } \rho_K = 0 \tag{17}$$

Eq. 17 limits the axial stress at the ultimate strain of FRP-confined concrete f_{cu}' to a minimum value of $0.85 f_{co}'$, because the concrete is deemed to have failed at this stress level, regardless of whether the FRP jacket has failed by rupture or not. Moreover, it is proposed that if the value of f_{cu}' predicted by Eq. 14 is equal to or smaller than $0.85 f_{co}'$, the concrete should be taken as unconfined. In such cases, the values of f_{cu}' and ε_{cu} in Eq. 16 should be taken as $0.85 f_{co}'$ and 0.0035, respectively.

It should be noted that Version II, schematically illustrated in Fig. 10, differs from Version I only for insufficiently confined concrete (i.e. with $\rho_K < 0.01$). In Fig. 11, the performance of both modified versions for two pairs of insufficiently confined specimens is shown. These specimens were confined with only 1 ply of GFRP. The first pair (specimens 20 and 21) had an unconfined concrete strength of 39.6 MPa, a confinement ratio of 0.079 and a confinement stiffness ratio of 0.0090; the corresponding values for the second pair (specimens 28 and 29) were 45.9 MPa, 0.067 and 0.0078. The predicted stress-strain curves were obtained using $\varepsilon_{co} = 0.002$.

Note that for the specimens of Fig. 11a, the confinement ratio is greater than the minimum value of 0.07 for sufficient confinement defined by Lam and Teng (2003), but for the specimens of Fig. 11b, the confinement ratio is smaller than 0.07. In both cases, the confinement stiffness ratios are smaller than the critical value of 0.01 as defined in the present study. The original model predicts a monotonically ascending stress-strain curve for

the specimens of Fig. 11a, but a stress-strain curve with a horizontal second portion for the specimens of Fig. 11b; the test curves are of the descending type in both cases. Version I of the modified Lam and Teng model predicts a horizontal second portion for specimens of both Figs 10a and 10b, which does not match the test curves well but provides a reasonably close approximation. By contrast, Version II of the modified Lam and Teng model is capable of predicting a descending branch and shows improved agreement with the test stress-strain curves.

8   Conclusions

This paper has presented the results of a recent study aimed at the refinement of the design-oriented stress-strain model for FRP-confined concrete originally developed by Lam and Teng (2003). Some weaknesses of this model have been illustrated through comparisons with recent test results obtained at The Hong Kong Polytechnic University. New equations for predicting the ultimate axial strain and the compressive strength of FRP-confined concrete have been developed based on the interpretation of these test results and results from a parametric study using a recent analysis-oriented stress-strain model (Teng et al. 2007a, Jiang and Teng 2007). Two modified versions of Lam and Teng's (2003) model have been proposed. Version I involves only the updating of the ultimate axial strain and compressive strength equations. Version II is capable of predicting stress-strain curves with a descending branch, which is not catered for by the original model of Lam and Teng (2003). The following conclusions can be drawn from the present study:

1. The original model of Lam and Teng (2003) overestimates the ultimate strain of concrete confined with a large amount of FRP and the compressive strength of concrete confined with a small amount of FRP.

2. The new ultimate strain and compressive strength equations account for the effects of confinement stiffness and jacket strain capacity separately and provide close predictions of test results.

3. Both modified versions of Lam and Teng's model provide much closer predictions of test stress-strain curves than the original model. Version II performs better than Version I for test stress-strain curves with a descending branch, although Version I also provides a reasonably close approximation of such test stress-strain curves.

4. Both modified versions are suitable for direct use in practical design and for inclusion in design codes/specifications. Version I is more compatible with most current design codes for concrete structures as the second portion of the predicted stress-strain curve reduces naturally to a horizontal line for unconfined concrete.

References

ACI-318 (2005). *Building Code Requirements for Structural Concrete and Commentary*, American Concrete Institute, Farmington Hills, Michigan, USA.

ACI-440.2R (2008). *Guide for the Design and Construction of Externally Bonded FRP Systems for Strengthening Concrete Structures*, American Concrete Institute, Farmington Hills, Michigan, USA.

Berthet, J.F., Ferrier, E. and Hamelin, P. (2006). "Compressive behavior of concrete externally confined by composite jackets - Part B: modeling", *Construction and Building Materials*, 20(5), 338-347.

Binici, B. (2005). "An analytical model for stress–strain behavior of confined concrete", *Engineering Structures,* 27(7), 1040-1051.

BS 8110 (1997). *Structural Use of Concrete*, Part 1, Code of practice for design and construction, British Standards Institution, London, UK.

Carey, S.A. and Harries, K.A. (2005). "Axial behavior and modeling of confined small-, medium-, and large-scale circular sections with carbon fiber-reinforced polymer jackets", *ACI Structural Journal*, 102 (4), 596-604.

Concrete Society (2004). *Design Guidance for Strengthening Concrete Structures with Fibre Composite Materials*. Concrete Society Technical Report No. 55, 2nd Edition, Crowthorne, Berkshire, UK.

Chun, S.S. and Park, H.C. (2002). "Load carrying capacity and ductility of RC columns confined by carbon fiber reinforced polymer." *Proceedings, 3rd International Conference on Composites in Infrastructure* (CD-Rom), San Francisco.

ENV 1992-1-1 (1991). *Eurocode 2: Design of Concrete Structures – Part 1: General Rules and Rules for Buildings*, European Committee for Standardization, Brussels.

Fam, A.Z. and Rizkalla, S.H. (2001). "Confinement model for axially loaded concrete confined by circular fiber-reinforced polymer tubes", *ACI Structural Journal*, 98(4), 451-461.

Fardis, M.N. and Khalili, H. (1982). "FRP-encased concrete as a structural material", *Magazine of Concrete Research*, 34(122), 191-202.

Harries, K.A. and Kharel, G. (2002). "Behavior and modeling of concrete subject to variable confining pressure", *ACI Materials Journal*, 99(2), 180-189.

Hognestad, E. (1951). *A Study of Combined Bending and Axial Load in Reinforced Concrete Members*, Bulletin Series No. 399, Engineering Experiment Station, University of Illinois, Urbana, Ill.

Karbhari, V.M. and Gao, Y. (1997). "Composite jacketed concrete under uniaxial compression–verification of simple design equations", *Journal of Materials in Civil Engineering,* ASCE, 9(4), 185-193.

Jiang, T., and Teng, J.G. (2007). "Analysis-oriented models for FRP-confined concrete: a comparative assessment", *Engineering Structures*, 29 (11), 2968-2986.

Lam, L., and Teng, J.G. (2003). "Design-oriented stress-strain model for FRP-confined concrete", *Construction and Building Materials*, 17(6-7), 471-489.

Lam, L., and Teng, J.G. (2004). "Ultimate condition of fiber reinforced polymer-confined concrete", *Journal of Composites for Construction*, ASCE, 8(6), 539-548.

Lam, L., Teng, J.G., Cheng, C.H. and Xiao, Y. (2006). "FRP-confined concrete under axial cyclic compression", *Cement and Concrete Composites*, 28(10), 949-958.

Lillistone, D. and Jolly, C.K. (2000). "An innovative form of reinforcement for concrete columns using advanced composites", *The Structural Engineer*, 78(23/24), 20-28.

Marques, S.P.C., Marques, D.C.S.C., da Silva J.L. and Cavalcante, M.A.A. (2004). "Model for analysis of short columns of concrete confined by fiber-reinforced polymer", *Journal of Composites for Construction*, ASCE, 8(4), 332-340.

Mattys, S., Toutanji, H., Audenaert, K. and Taerwe, L. (2005). "Axial behavior of large-scale columns confined with fiber-reinforced polymer composites", *ACI Structural Journal*, 102(2), 258-267.

Mirmiran, A. and Shahawy, M. (1997). "Dilation characteristics of confined concrete", *Mechanics of Cohesive-Frictional Materials*, 2 (3), 237-249.

Miyauchi, K., Inoue, S., Kuroda, T. and Kobayashi, (1999). "Strengthening effects of concrete columns with carbon fiber sheet", *Transactions of the Japan Concrete Institute*, 21, 143-150.

Popovics, S. (1973). "Numerical approach to the complete stress-strain relation for concrete", *Cement and Concrete Research*, 3(5), 583-599.

Rocca, S., Galati, N. and Nanni, A. (2006). "Large-size reinforced concrete columns strengthened with carbon FRP: experimental evaluation", *Proceedings, 3rd International Conference on FRP Composites in Civil Engineering*, December 13-15 2006, Miami, Florida, USA.

Saafi, M., Toutanji, H.A. and Li, Z. (1999). "Behavior of concrete columns confined with fiber reinforced polymer tubes", *ACI Materials Journal*, 96(4), 500-509.

Samaan, M., Mirmiran, A., and Shahawy, M. (1998). "Model of concrete confined by fiber composite", *Journal of Structural Engineering*, ASCE, 124(9), 1025-1031.

Saenz, N. and Pantelides, C.P. (2007). "Strain-based confinement model for FRP-confined concrete", *Journal of Structural Engineering*, ASCE, 133 (6), 825-833.

Spoelstra, M.R., and Monti, G. (1999). "FRP-confined concrete model", *Journal of Composites for Construction*, ASCE, 3(3), 143-150.

Teng, J.G., and Lam, L. (2004). "Behavior and modeling of fiber reinforced polymer-confined concrete", *Journal of Structural Engineering*, ASCE, 130(11), 1713-1723.

Teng, J.G., Huang, Y.L., Lam, L., and Ye, L.P. (2007a). "Theoretical model for fiber reinforced polymer-confined concrete", *Journal of Composites for Construction*, ASCE, 11(2), 201-210.

Teng, J.G., Yu, T., Wong, Y.L., and Dong, S.L. (2007b). "Hybrid FRP-concrete-steel tubular columns: concept and behavior", *Construction and Building Materials*, 21(4), 846-854.

Toutanji, H.A. (1999). "Stress-strain characteristics of concrete columns externally confined with advanced fiber composite sheets", *ACI Materials Journal*, 96(3), 397-404.

Wu, G., Wu, Z.S. and Lu, Z.T. (2007). "Design-oriented stress-strain model for concrete prisms confined with FRP composites", *Construction and Building Materials*, 21(5), 1107-1121.

Xiao, Y. and Wu, H. (2000). "Compressive behavior of concrete confined by carbon fiber composite jackets." *Journal of Materials in Civil Engineering*, ASCE, 12(2), 139-146.

Xiao, Y. and Wu, H. (2003). "Compressive behavior of concrete confined by various types of FRP composites jackets." Journal of Reinforced Plastics and Composites, 22(13), 1187-1202.

Yeh, F.Y. and Chang, K.C. (2007). "Confinement efficiency and size effect of FRP confined circular concrete columns", *Structural Engineering and Mechanics*, 26(2), 127-150.

Youssef, M.N. (2003). *Stress-strain Model for Concrete Confined by FRP Composites*, Ph.D. Dissertation, University of California, Irvine.

Youssef, M.N., Feng, M.Q. and Mosallam, A.S. (2007). "Stress-strain model for concrete confined by FRP composites", *Composites Part B – Engineering*, 38(5-6), 614-628.

Table 1 Properties of test specimens used in this paper

Source	Specimen	D (mm)	H (mm)	$f_{co}^{'}$ (MPa)	ε_{co} (%)	Fiber type	t (mm)	E_{frp} (GPa)	$\varepsilon_{h,rup}$ (%)	$f_{cc}^{'}$ ($f_{cu}^{'}$) (MPa)	ε_{cu} (%)
Lam et al. (2006)	17	152	305	38.9	0.250	Carbon	0.33	247	1.060	76.8	1.910
	18	152	305	38.9	0.250	Carbon	0.33	247	1.130	79.1	2.080
	19	152	305	38.9	0.250	Carbon	0.33	247	0.790	65.8	1.250
Teng et al. (2007b)	20	152	305	39.6	0.263	Glass	0.17	80.1	1.869	41.5 (38.8)	0.825
	21	152	305	39.6	0.263	Glass	0.17	80.1	1.609	40.8 (37.2)	0.942
	22	152	305	39.6	0.263	Glass	0.34	80.1	2.040	54.6	2.130
	23	152	305	39.6	0.263	Glass	0.34	80.1	2.061	56.3	1.825
	24	152	305	39.6	0.263	Glass	0.51	80.1	1.955	65.7	2.558
	25	152	305	39.6	0.263	Glass	0.51	80.1	1.667	60.9	1.792
Jiang and Teng (2007)	28	152	305	45.9	0.243	Glass	0.17	80.1	1.523	48.4 (40.5)	0.813
	29	152	305	45.9	0.243	Glass	0.17	80.1	1.915	46.0 (40.5)	1.063
	31	152	305	45.9	0.243	Glass	0.34	80.1	1.799	55.2	1.254
	34	152	305	38.0	0.217	Carbon	0.68	240.7	0.977	110.1	2.551
	35	152	305	38.0	0.217	Carbon	0.68	240.7	0.965	107.4	2.613
	38	152	305	38.0	0.217	Carbon	1.36	240.7	0.872	161.3	3.700
	39	152	305	38.0	0.217	Carbon	1.36	240.7	0.877	158.5	3.544
	42	152	305	44.2	0.260	Carbon	0.11	260	0.734	48.1	0.691
	45	152	305	44.2	0.260	Carbon	0.22	260	0.938	62.9	1.025

Table 2 Parameters used in the parametric study

Concrete	$f_{co}^{'}$ (MPa)	20 to 50 at an interval of 5
CFRP	E_{frp} (GPa)	230
	$\varepsilon_{h,rup}$	0.0075
	t (mm)	0 to 1 at an interval of 0.1
GFRP	E_{frp} (GPa)	80
	$\varepsilon_{h,rup}$	0.015
	t (mm)	0 to 1.5 at an interval of 0.1
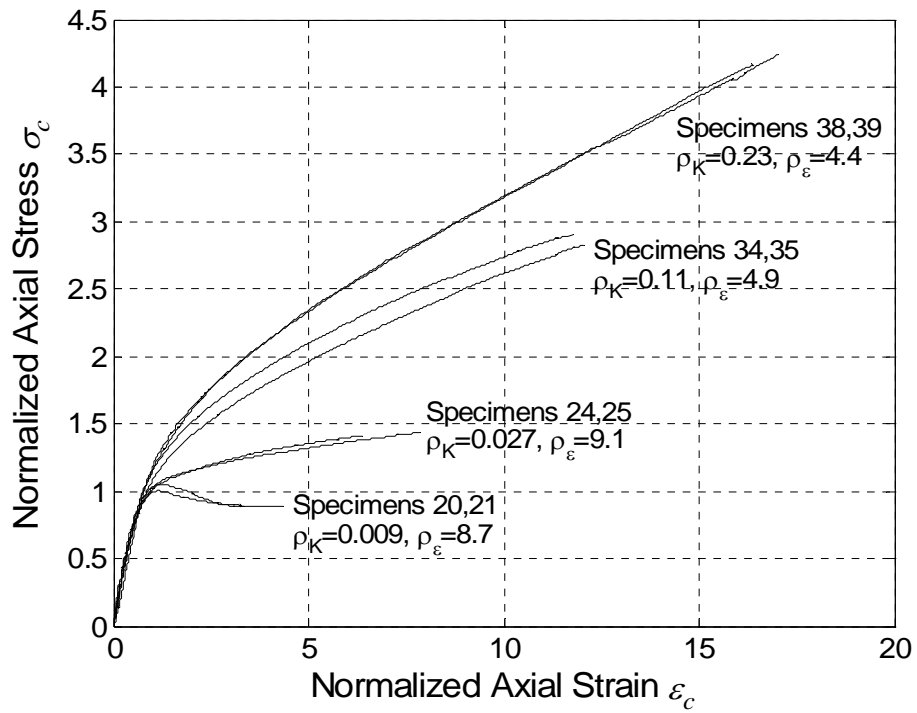
(a) Axial stress-axial strain curves
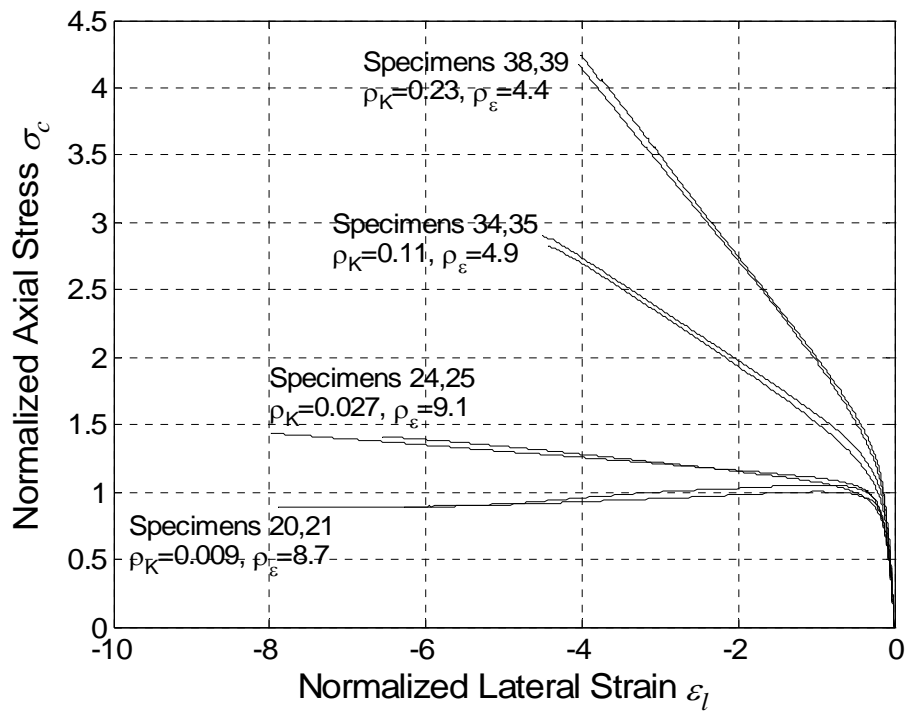
(b) Axial stress-lateral strain curves

Fig. 1 Typical stress-strain behavior of FRP-confined concrete cylinders

17
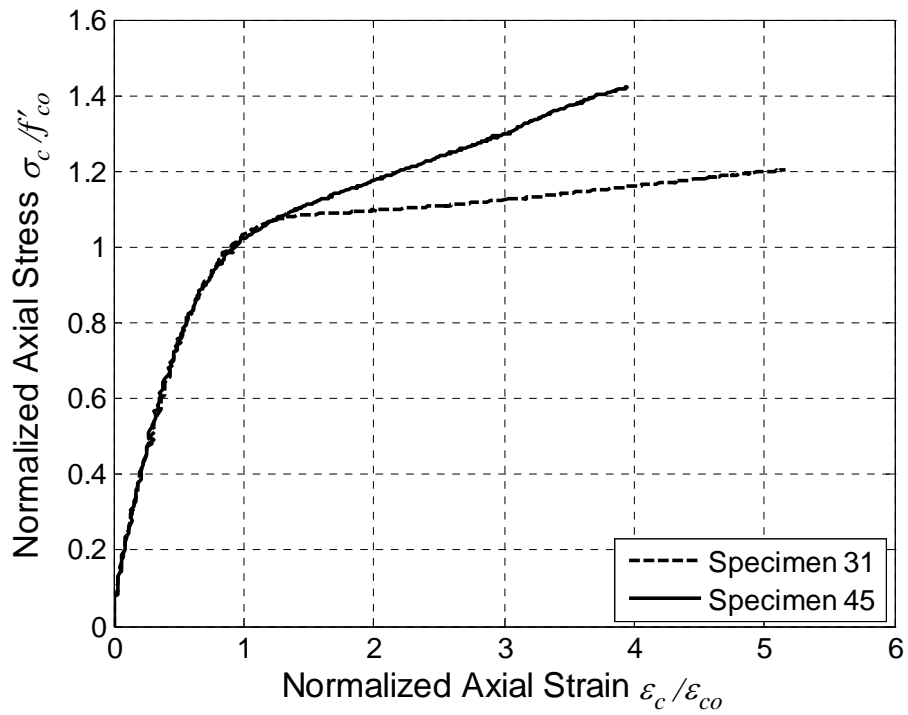
(a) Comparison between specimen 31 and specimen 45
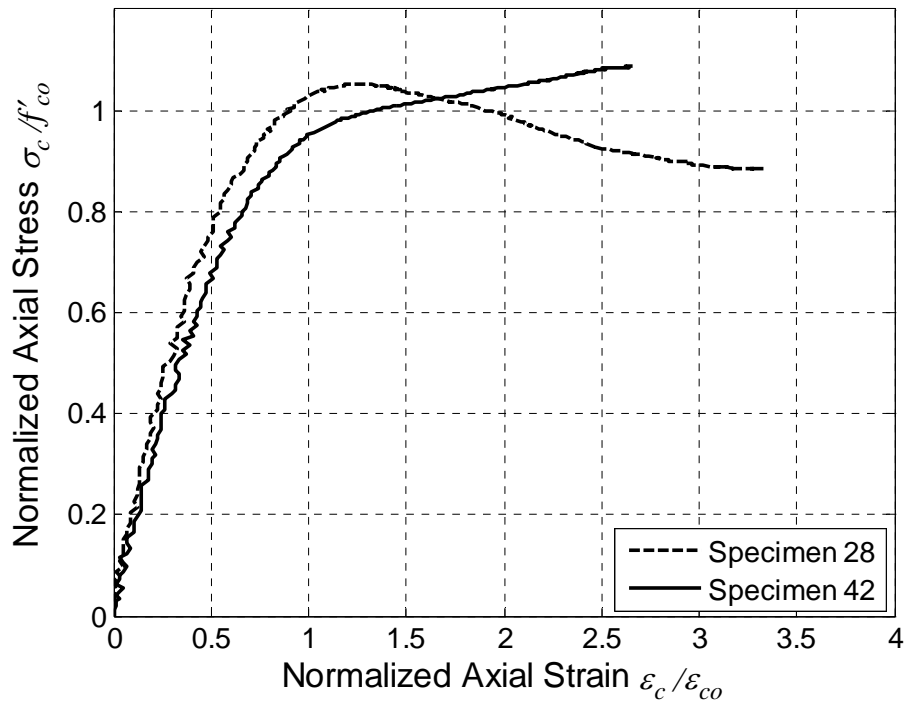
(b) Comparison between specimen 28 and specimen 42

Fig. 2 Effect of confinement stiffness on stress-strain behavior of

FRP-confined concrete
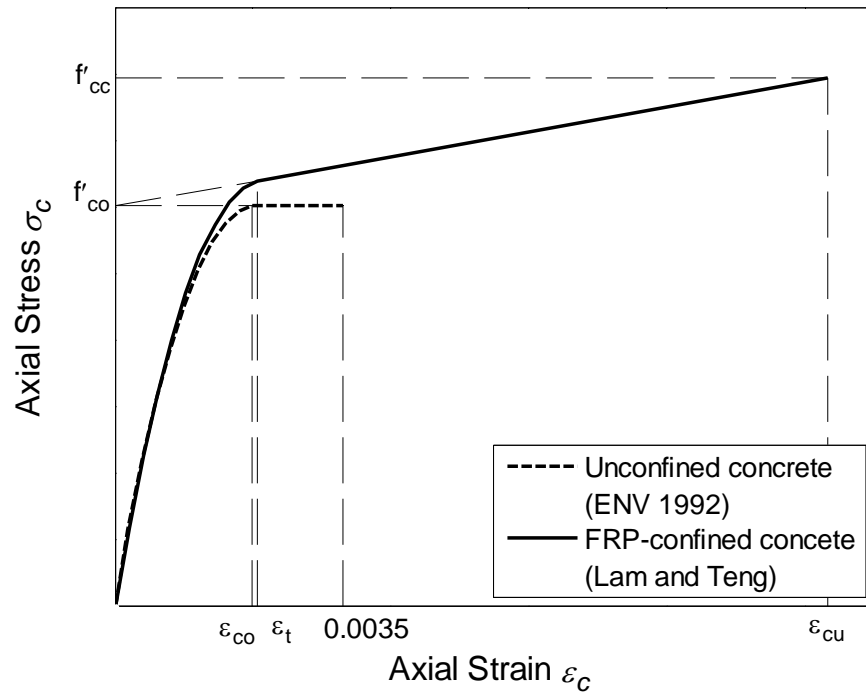
Fig. 3 Illustration of Lam and Teng's model
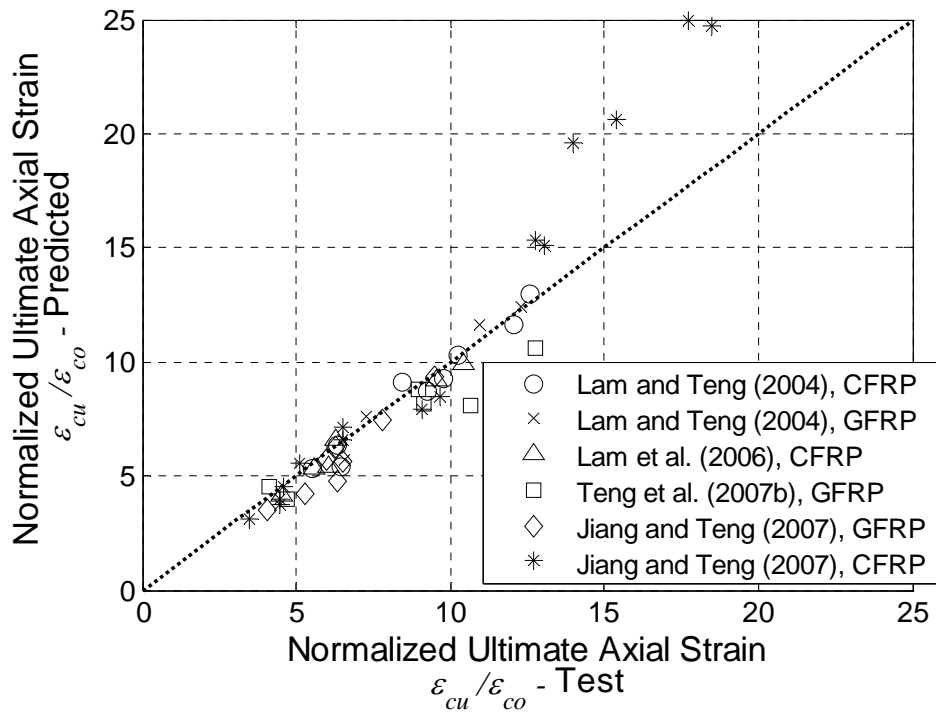
(a) Ultimate axial strain
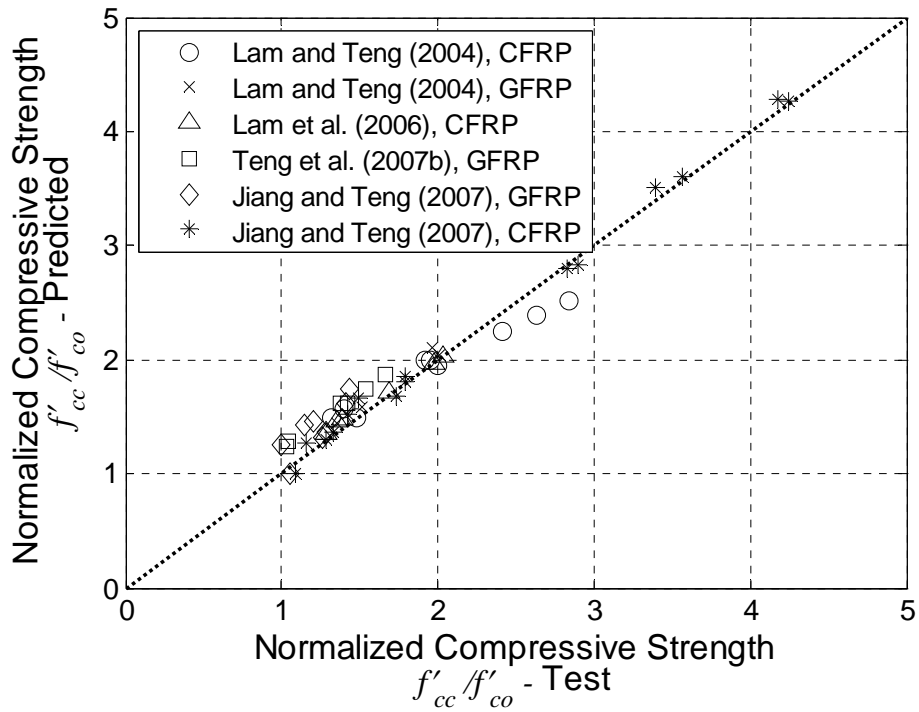
(b) Compressive strength

Fig.4 Performance of Lam and Teng' s model against the present test results
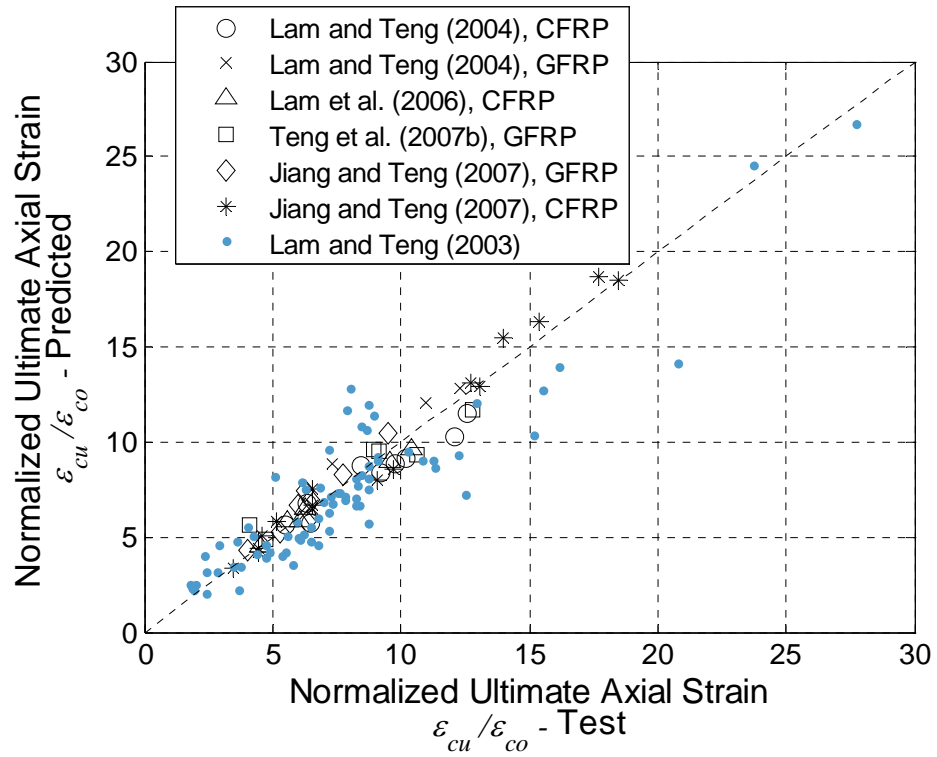
Fig. 5 Performance of Eq. 9
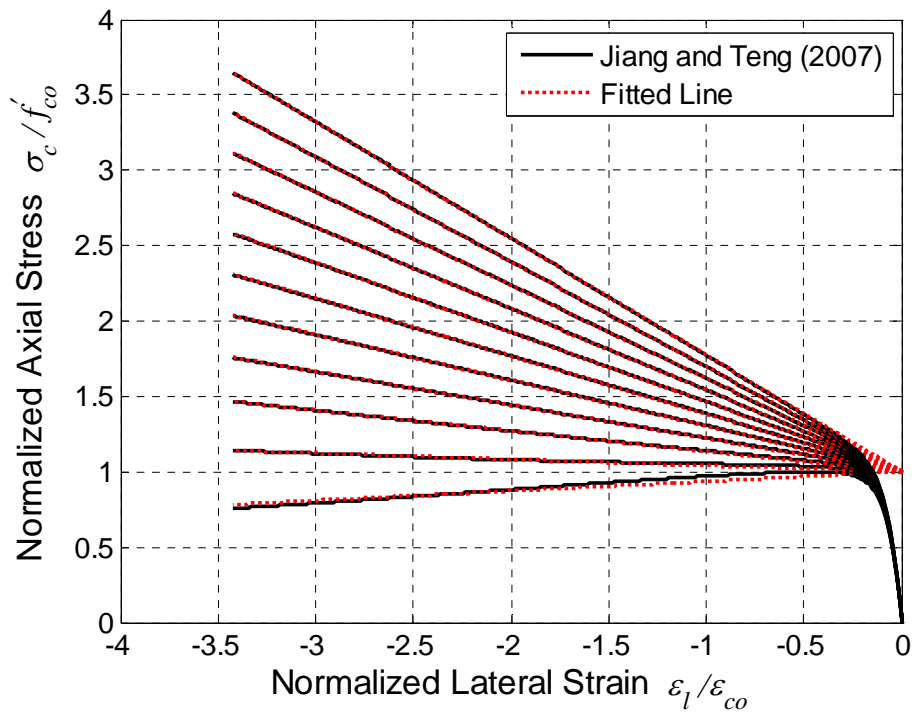
(a) First two steps
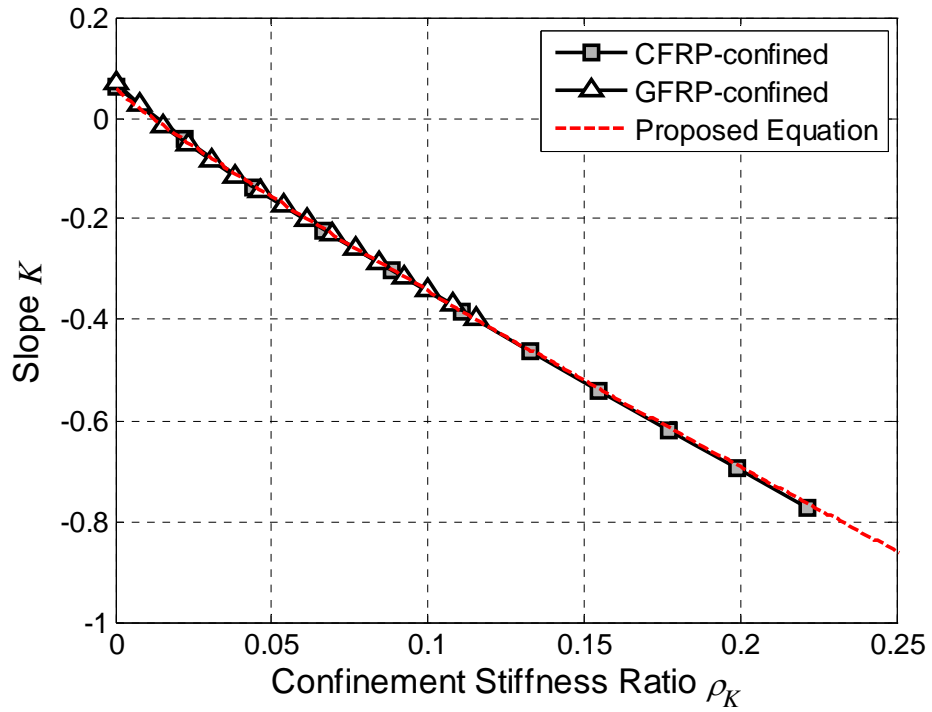
(b) Last step

Fig. 6 Demonstration of the parametric study
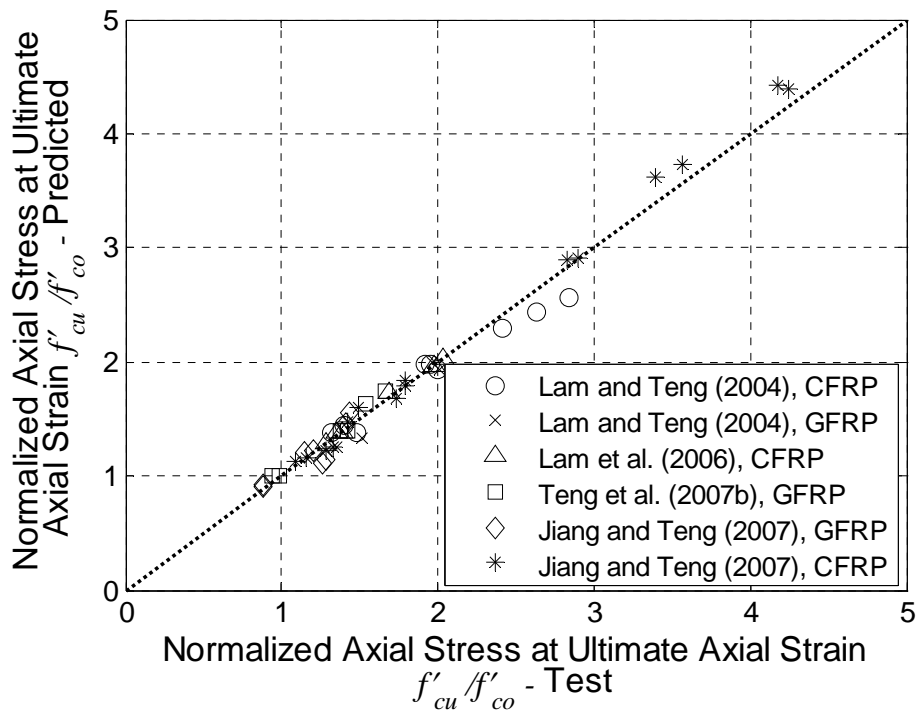
Fig. 7 Performance of Eq. 13
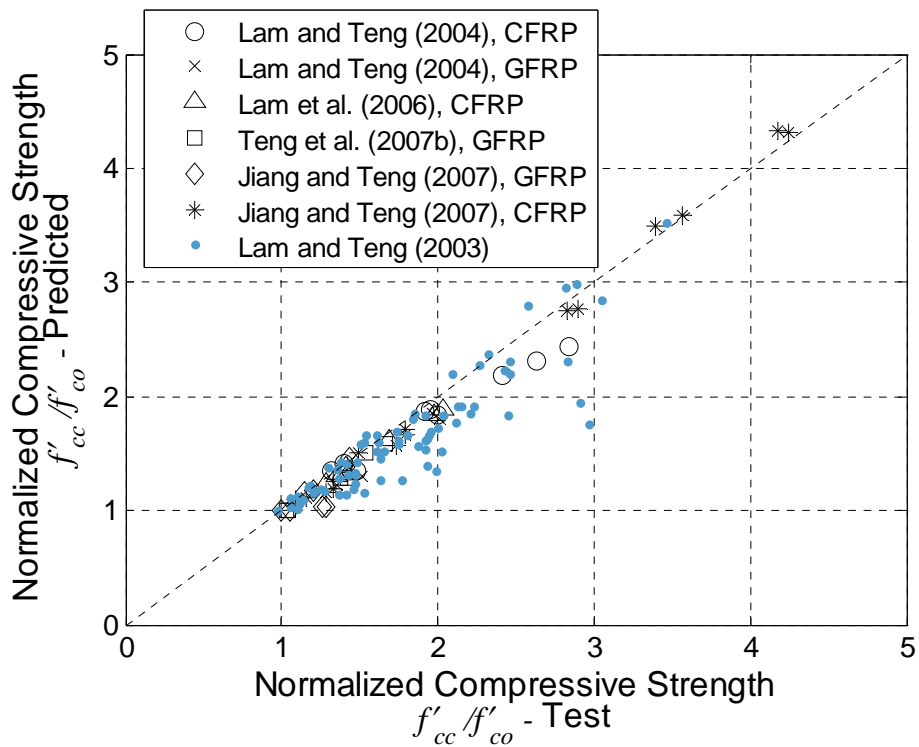
Fig. 8 Performance of Eq. 15
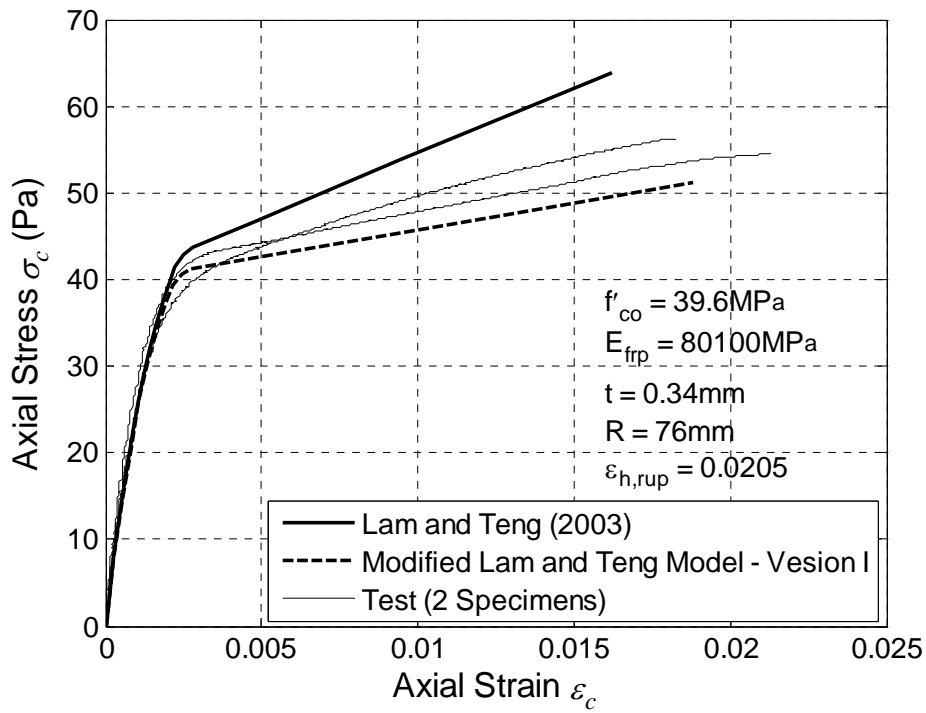
(a) Specimens 22 and 23
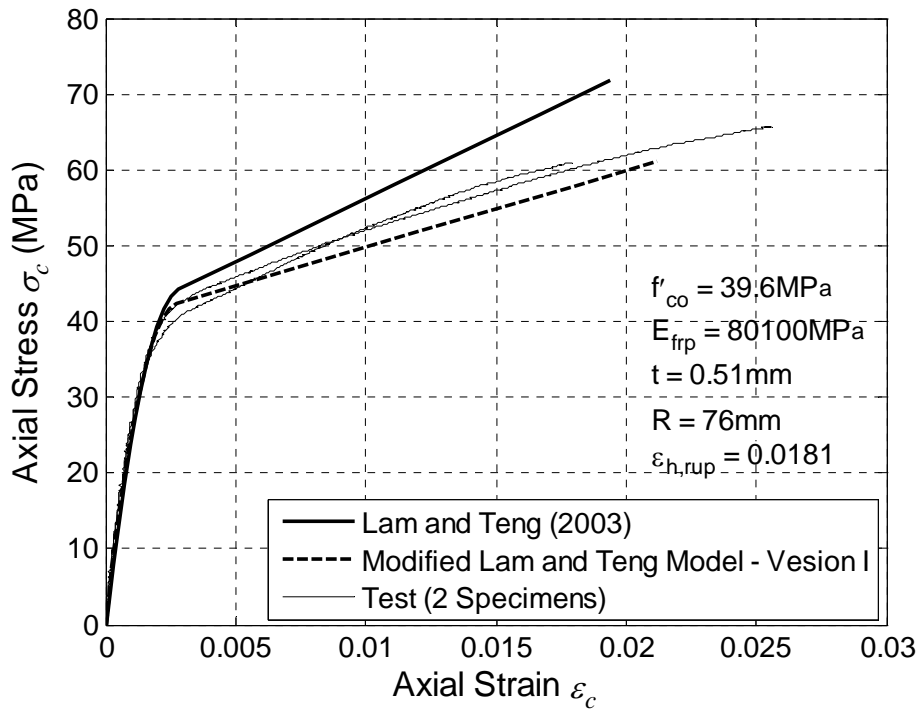
(b) Specimens 24 and 25
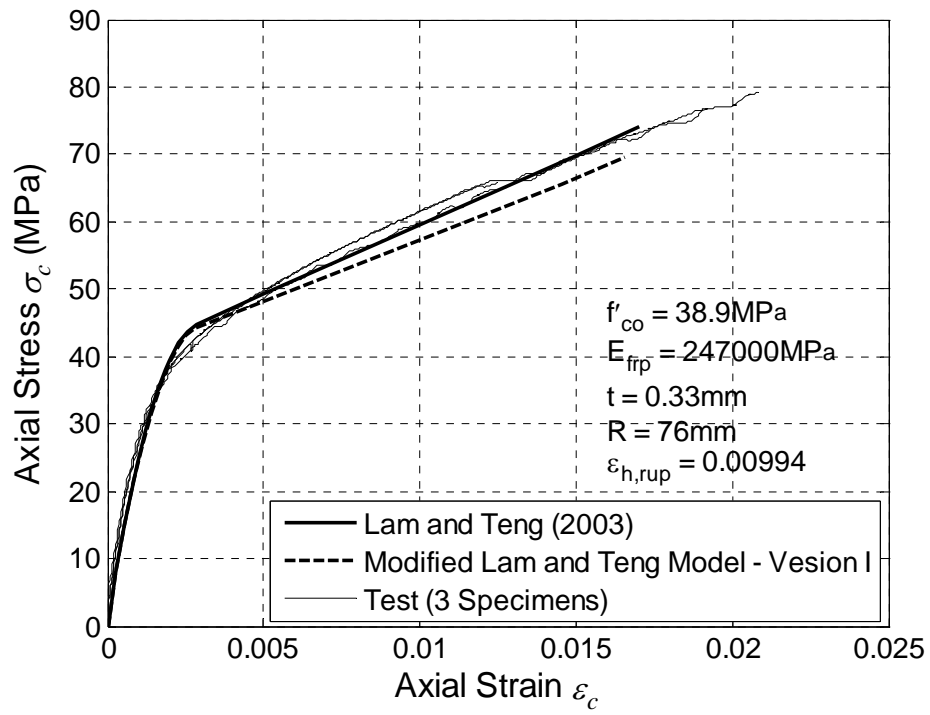
(c) Specimens 17,18 and 19

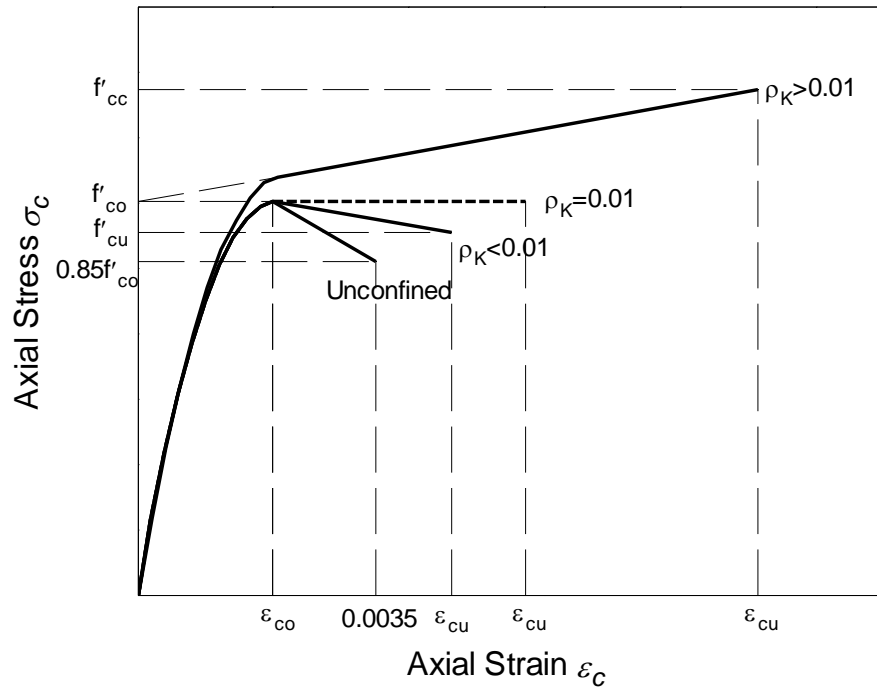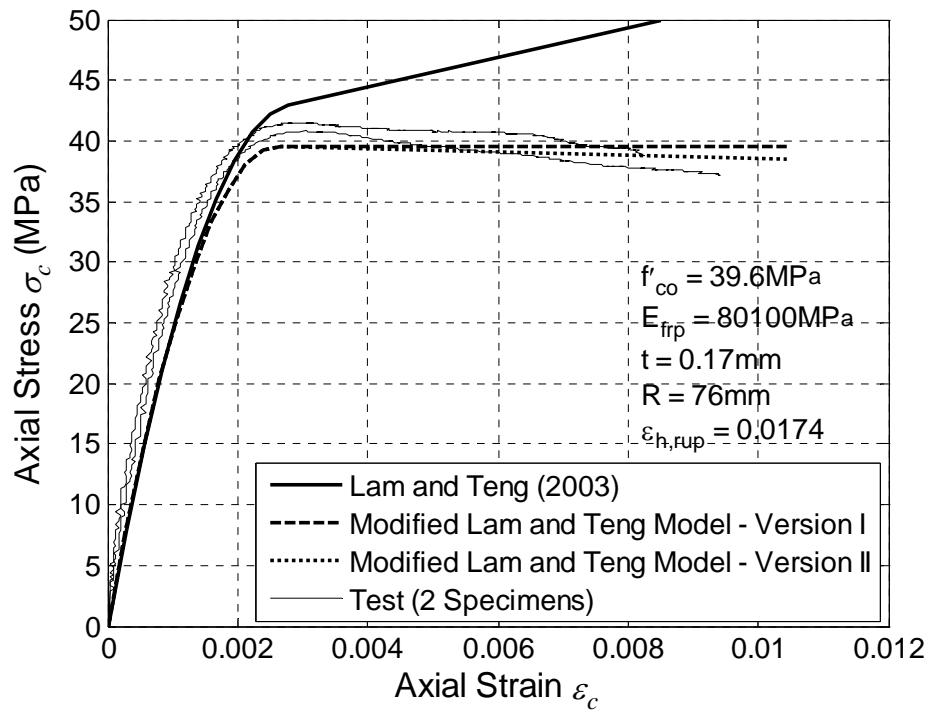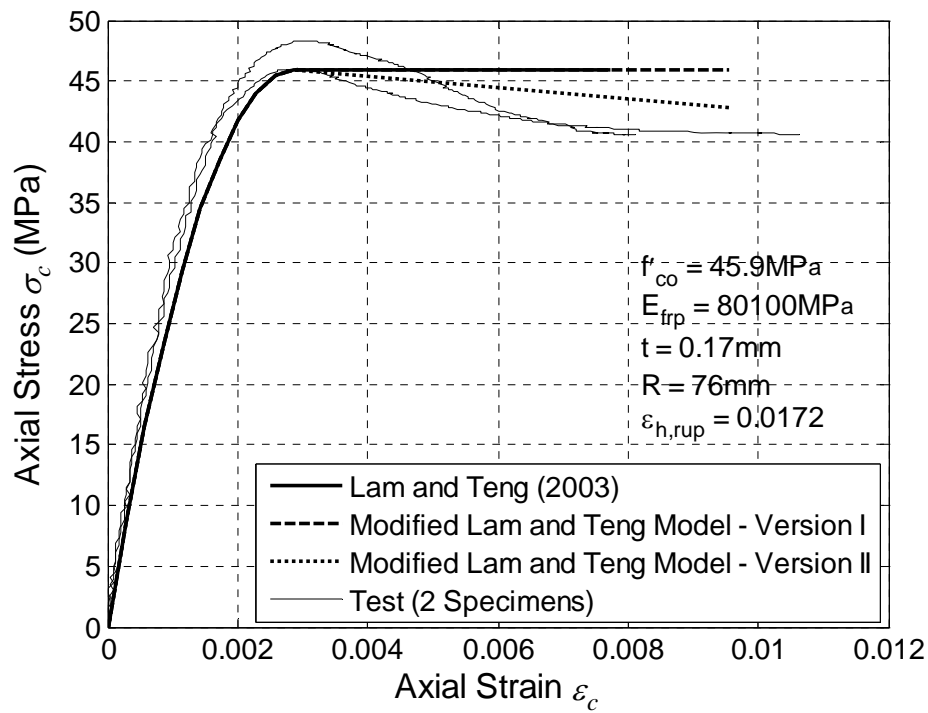Fig. 9 Performance of Version I of the modified Lam and Teng model

Fig. 10 Schematic of Version II of the modified Lam and Teng model

(a) Specimens 20 and 21

(b) Specimens 28 and 29

Fig. 11 Prediction of decreasing type of stress-strain curves